RESEARCH ARTICLE

Shifts in coastal Antarctic marine microbial communities during and after melt water-related surface stratification

Anouk M.-T. Piquet[1], Henk Bolhuis[2], Michael P. Meredith[3] & Anita G.J. Buma[1]

[1]Department of Ocean Ecosystems, Energy and Sustainability Research Institute, University of Groningen, Groningen, The Netherlands; [2]Department of Marine Microbiology, NIOO-CEME, NT Yerseke, The Netherlands; and [3]British Antarctic Survey, NERC, High Cross, Cambridge, UK

Correspondence: Anouk M.-T. Piquet, Department of Ocean Ecosystems, Energy and Sustainability Research Institute, University of Groningen, Nijenborgh 7, 9747 AG Groningen, The Netherlands. Tel.: +31 50 363 2286; fax: +31 50 363 2261; e-mail: a.m.t.piquet@rug.nl

Received 18 June 2010; revised 17 January 2011; accepted 26 January 2011.
Final version published online 14 March 2011.

DOI:10.1111/j.1574-6941.2011.01062.x

Editor: Gary King

Keywords
Antarctic Peninsula; 18S rRNA gene; 16S rRNA gene; bacterioplankton; DGGE; sequencing.

Abstract

Antarctic coastal waters undergo major physical alterations during summer. Increased temperatures induce sea-ice melting and glacial melt water input, leading to strong stratification of the upper water column. We investigated the composition of micro-eukaryotic and bacterial communities in Ryder Bay, Antarctic Peninsula, during and after summertime melt water stratification, applying community fingerprinting (denaturing gradient gel electrophoresis) and sequencing analysis of partial 18S and 16S rRNA genes. Community fingerprinting of the eukaryotic community revealed two major patterns, coinciding with a period of melt water stratification, followed by a period characterized by regular wind-induced breakdown of surface stratification. During the first stratified period, we observed depth-related differences in eukaryotic fingerprints while differences in bacterial fingerprints were weak. Wind-induced breakdown of the melt water layer caused a shift in the eukaryotic community from an *Actinocyclus* sp.- to a *Thalassiosira* sp.-dominated community. In addition, a distinct transition in the bacterial community was found, but with a few days' delay, suggesting a response to the changes in the eukaryotic community rather than to the mixing event itself. Sequence analysis revealed a shift from an *Alpha-* and *Gammaproteobacteria* to a *Cytophaga–Flavobacterium–Bacteroides*-dominated community under mixed conditions. Our results show that melt water stratification and the transition to nonstabilized Antarctic surface waters may have an impact not only on micro-eukaryotic but also bacterial community composition.

Introduction

Antarctic marine microbial communities inhabit water masses that are characterized by extreme and highly variable physical conditions. Especially in the Antarctic coastal and marginal ice zone regions, temperature and irradiation regimes are highly variable. Wind-mediated deep vertical mixing and sea-ice cover strongly reduce the average underwater irradiance regime available for marine organisms. This is contrasted with periods of the summer melting of sea ice or glaciers from nearby land masses reducing the surface water salinity and density, resulting in water column stratification and increased irradiance levels in shallow surface waters (Kang *et al.*, 2001; Dierssen *et al.*, 2002). In the Antarctic region, periods of water column stratification are associated with the development of phytoplankton blooms (Mura *et al.*, 1995; Moline & Prézelin, 1996; Kang *et al.*, 2001; Dierssen *et al.*, 2002). Taxonomic surveys between stratified and deeply mixed Antarctic water masses have shown that diatoms generally dominate under stratified conditions, while nanoflagellates dominate in deeply mixed waters (Arrigo *et al.*, 1999; Kang *et al.*, 2001). The effects of water column stabilization on marine microbial community structure have so far been mainly conducted on marine microalgae, applying microscopic or specific pigment analyses. In contrast, the effect of stratification on bacteria remains relatively understudied.

Although still lagging behind the large number of studies on marine prokaryotic diversity (Ferrari & Hollibaugh, 1999; Massana *et al.*, 2001; Schäfer *et al.*, 2001; Casamayor *et al.*, 2002; Riemann *et al.*, 2008), the application of molecular tools in the study of marine protist community

composition has gradually gained more momentum (e.g. Beszteri *et al.*, 2005; Richards & Bass, 2005; Piquet *et al.*, 2008, 2010). Different molecular tools have been implemented in diversity studies on marine protists, using the 18S rRNA gene and methods such as denaturing gradient gel electrophoresis (DGGE). Based on these approaches, samples collected from different oceanic regions including the Pacific, Atlantic and Southern Oceans revealed unexpected high diversities for the smaller-sized ($< 5\,\mu m$) eukaryotes (López-García *et al.*, 2001; Moreira & López-García, 2002; Moon-van der Staay *et al.*, 2003; Massana *et al.*, 2004; Richards & Bass, 2005). Currently, increasing numbers of unique environmental sequences are being uncovered, revealing novel lineages among the Alveolates, Stramenopiles and Prasinophytes (Moreira & López-García, 2002; Massana *et al.*, 2004; Guillou *et al.*, 2005). Only a limited number of studies have used DGGE to describe micro-eukaryotic diversity and succession at marine Antarctic sites (Díez *et al.*, 2001; Gast *et al.*, 2004).

In the present study, we assessed the surface micro-eukaryotic (2–200 μm size) and bacterial communities applying DGGE and cloning-sequencing analysis, during and after summertime surface stratification in Ryder Bay, Antarctic Peninsula. We hypothesized that changes in surface sea water properties, either stratified by melt water input or (temporarily) mixed by wind, would shape the eukaryotic as well as the bacterial community composition. Whereas the micro-eukaryotes may be directly affected by the extant conditions, the prokaryotes, which play an important role in the recycling of organic matter, may be indirectly affected by following the shifts in the micro-eukaryotic community composition, similar to the bacterial response on algal blooms (Billen & Becquevort, 1991).

Materials and methods

This study was carried out in Ryder Bay (67°34′S, 68°08′W) near the Rothera research station [British Antarctic Survey (BAS)] located on Adelaide Island at the western Antarctic Peninsula, between January 20 (Julian day 20: *Jd*. 20) and February 28 (*Jd*. 59), 1998. Water column characteristics and ice coverage were studied in collaboration with the Rothera Oceanographic and Biological Time Series [RaTS; see http://www.antarctica.ac.uk/rats; (Clarke *et al.*, 2008)]. Water column profiling was conducted using a Chelsea Instruments Aquapack Conductivity–Temperature–Depth (CTD) probe, with an integrated fluorometer. CTD salinity was calibrated following an intercomparison with high-precision salinity measurements made with shipboard CTD profilers; the latter were calibrated using IAPSO P-series standard seawater. Chlorophyll concentrations were derived from CTD fluorescence following calibration against discrete samples that were collected throughout the year at 15 m depth and analyzed for size-fractionated and total chlorophyll concentration [see Clarke *et al.* (2008) for full details].

Water samples were collected at three depths (0, 5 and 10 m) on six dates, using 5-L Niskin bottles. These dates were January 20 (*Jd.* 20), January 28 (*Jd.* 28), January 31 (*Jd.* 31), February 1 (*Jd.* 32), February 13 (*Jd.* 44) and February 27 (*Jd.* 58). Sampling day numbers, as presented in Figs 1–4, are given in parentheses. Surface samples were only taken on January 17 (*Jd.* 17), January 19 (*Jd.* 19), January 26 (*Jd.* 26), February 5 (*Jd.* 36), February 12 (*Jd.* 43), February 19 (*Jd.* 59), February 26 (*Jd.* 57), as well as on March 1 (*Jd.* 60) and March 5 (*Jd.* 64). Samples were transported immediately to the laboratory, where between 1 and 3 L of water was size fractionated over Poretics membrane filters (Osmonics, Livermore, CA) of various pore sizes (0.2, 2 and 10 μm). Filters were frozen at $-20\,^{\circ}C$ until further analysis. More details on the sampling strategy, environmental data collection and DNA extraction procedure are given in Buma *et al.* (2001). Samples were coded using the sampling day numbers (as given above), the collection depth (m) and size fraction (μm). DNA was extracted using the standard cetyltrimethylammonium bromide method (Doyle & Doyle, 1987) and subsequently stored at $-80\,^{\circ}C$. In addition to the CTD measurements, discrete salinity measurements for later principal component analysis were performed in the Lugol-fixed subsamples that were used in Buma *et al.* (2001) for taxonomic composition analysis using classical microscopy. Earlier, Lugol fixation had been shown (Buma *et al.*, 2001) not to significantly affect salinity measurements (variability with nonfixed samples < 0.1 PSU, which was considered acceptable for the present study). Wind speed data were provided by the BAS meteorological station.

Molecular analysis

DNA obtained from the > 10 and 10–2 μm size fractions were used to analyze the eukaryotic community and DNA from the 2–0.2 μm size fraction for analysis of the bacterial community. Because of the occasional DNA shortage, often resulting from earlier use of DNA extracts for CPD analysis (Buma *et al.*, 2001), not all samples could be processed for molecular analysis, resulting in the absence of some depth and size fractions in our presentation. Molecular analysis of the eukaryotic and bacterial community was performed on partial fragments of the 18S and 16S rRNA genes, respectively. Although differences in rRNA gene copy numbers between species or primer annealing differences can induce biases in the amplified fragments, the application of PCR on environmental samples is widely used in the field of microbial and molecular ecology (Suzuki & Giovannoni, 1996; Speksneijder *et al.*, 2001; Frey *et al.*, 2006). We applied a combination of partial amplification of the rRNA genes,

subsequent DGGE and clone library sequencing for community profiling and species identification.

A 500-bp fragment of the 18S rRNA gene was amplified using the eukaryote-specific primer set Euk1A and 516r-GC (Díez *et al.*, 2001). Amplification procedures were performed as described in Piquet *et al.* (2008). Approximately 430 bp of the variable V6 region of the 16S rRNA gene was amplified using the universal bacterial primers U968f-GC forward primer, containing a GC clamp at the 5′end, and the U1401R reverse primer (Nübel *et al.*, 1996). The PCR program used for 16S rRNA gene amplification started with a 5-min 94 °C denaturation step, 10 touchdown cycles, where the annealing temperature was decreased by 0.5 °C each cycle, providing a gradient from 60 to 55 °C, and a further 25 cycles of 60-s denaturing at 94 °C, 60-s annealing at 55 °C and 120-s extension at 72 °C. The amplification was finalized by a final extension step of 72 °C for 30 min to remove artificial double bands (Janse *et al.*, 2004). PCR products were separated by DNA gel-electrophoresis on a 1% agarose gel, stained with ethidium bromide and visualized using an Image Master (Pharma Biotech). Amplicon yield was estimated by comparing the bands with a DNA Smart Ladder (Eurogentec).

PCR products of expected size and quantity were subjected to DGGE analysis using the PhorU system (Ingeny). Two hundred nanograms of each PCR amplicon were run on DGGE with 40–70% and 10–60% denaturing gradients for the 16S and 18S rRNA gene amplicons, respectively. Band patterns were translated into presence/absence data, analyzed with the Dice similarity coefficient and presented in the form of an unweighted pair group method with arithmetic averages dendrogram using the BIONUMERICS software package (Applied Maths). The 18S rRNA gene DGGE bands identified as Metazoa (Table 1) were excluded from further statistical analysis. More details on the DGGE methods and analysis are given in Piquet *et al.* (2008).

Ordination analysis

We ran unimodal detrended correspondence analysis (DCA) and redundancy analysis (RDA) (Van den Wollenberg, 2007) with CANOCO version 4.5.2 (Ter Braak & Šmilauer, 1998) on the presence and absence of 42 bands of the 18S rRNA gene DGGE profiles and on the following environmental variables: salinity (as measured in Lugol-fixed samples), average wind speed, stratification (1 = stratified; 0 = not stratified), size fraction and sampling depth. For ordination analysis purposes, we defined 'stratified' using measured salinities and observed wind speeds: the upper (0–10 m) water column was considered stratified when surface salinity was < 32 psu and wind speeds were $< 5\,m\,s^{-1}$.

A similar analysis was performed on the presence and absence data of 30 bands from the 16S rRNA gene DGGE profiles. Subsequently, Monte Carlo's unrestricted permutation test (1000 permutations) was run on the data set to determine the significance of the environmental variables in explaining variation in the data set.

Species diversity

A subset of our samples, namely those that revealed larger differences in DGGE band patterns, were selected for further 18S rRNA gene sequence analysis. Clone libraries were generated from the remaining amplified DNA of the initial DGGE PCR amplicons obtained from the > 10-μm fraction of the following nine environmental samples: 22-0; 28-0; 28-10; 31-0; 31-10; 33-10; 41-0; 51-0; and 52-10 (coded by Julian day–depth). DNA fragments were cloned in pGEM-t (Promega) and transformed into chemically competent *Escherichia coli* strain JM109 (Promega) according to the manufacturer's protocol. Per sample, 40 positive inserts were selected, reamplified and rerun on a DGGE next to the original environmental sample PCR amplicon. Migration distances of the PCR products from the single clones were compared with the original environmental band patterns. Clones with the same migration lengths to bands of the environmental sample fingerprint were selected for subsequent sequencing. The pGEM-t inserts were reamplified from the vector's T7-SP6 sites, thereby providing the complete (500 bp) insert for sequencing. Amplification was followed by a cleanup step by polyethylene glycol 8000 (Sigma) precipitation. Sequence products were precipitated by adding 0.7 volume of isopropanol and were analyzed on an automated ABI 377 DNA sequencer according to the manufacturer's instructions (Applied Biosystems).

Samples of the smallest size fraction (0.2–2 μm) of surface samples: 22-0, 23-0, 23-10, 28-0, 42-5, 51-0 and 58-0 were selected for generating clone libraries. These samples were chosen because they showed a visible variation in the environmental DGGE band patterns. Nearly full-length 16S rRNA gene fragments were amplified from the environmental DNA using the universal bacterial primer set B8F (5′-AGAGTTTGATCMTGGCTCAG-3′)–U1406R (5′-ACGGG CGGTGTGTRC-3′). Amplification mixtures consisted of dNTP mix in a final concentration 200 μM, 200 nM primers, 1 × PCR buffer (GE Healthcare), 2.3 mM $MgCl_2$, 2% dimethyl sulfoxide, $0.2\,mg\,mL^{-1}$ bovine serum albumin (Roche) and 1 U Taq DNA polymerase (GE Helathcare). The reaction was run on a thermal cycler (GeneAmp®, PCR system 9700, Applied Biosystem) using the following program: 94 °C for 130 s; 35 cycles of 94 °C for 30 s, 56 °C for 45 s, 72 °C for 130 s; and a final elongation step of 72 °C for 7 min. From each sample, 96 colonies were picked and clones containing an insert (varying from 32 to 55 positive clones per sample) were sequenced in one direction. Sequencing was performed as described above, now using

Table 1. Eukaryote OTUs determined from clone sequencing and phylogenetic analysis

Group and OTU*	*N*†	DGGE id.‡	Closest BLAST match (accession number)§	Query/similarity¶	Closest cultivated BLAST match (accession no.)‖	Query/similarity¶
Stramenopiles						
ANT-Roth-MECl-2	3	Band 1	–	–	*Eucampia antarctica* (X85389)	535/535 (100%)
ANT-Roth-MECl-5	2	Band 2	–	–	*Chaetoceros rostratus* (X85391)	525/532 (98%)
ANT-Roth-MECl-4	1	Band 2	–	–	*Chaetoceros rostratus* (X85391)	510/532 (95%)
ANT-Roth-MECl-8	7	Band 3	–	–	*Actinocyclus curvatulus* (X85401)	533/534 (99%)
ANT-Roth-MECl-72	1	–	–	–	*Ditylum brightwellii* (FJ266034)	509/537 (94%)
ANT-Roth-MECl-10	1	Band 7	U. mar.euk. clone E1-43 (EU078279)	513/514 (99%)	*Nitzschia longissima* (AY881968)	508/524 (96%)
ANT-Roth-MECl-87	2	Band 7	–	–	*Fragilariopsis cylindrus* (EF140624)	511/516 (99%)
ANT-Roth-MECl-1	1	–	–	–	*Pseudo-nitzschia pungens* (NPU18240)	521/523 (99%)
ANT-Roth-MECl-33	4	–	–	–	*Pseudo-nitzschia pungens* (NPU18240)	519/523 (99%)
ANT-Roth-MECl-28	7	Band 8	–	–	*Thalassiosira tumida* (DQ514883)	532/537 (99%)
ANT-Roth-MECl-69	1	–	–	–	*Coscinodiscus* sp. (AY485448)	470/543 (85%)
ANT-Roth-MECl-66	1	–	–	–	*Porosira pseudodenticulata* (EU090015)	500/500 (100%)
Telonema sp.						
ANT-Roth-MECl-90	4	Band 10	U.euk. clone RA010412.17 (AJ564767)	530/542 (97%)	*Telonema subtilis* (AJ564772)	529/542 (97%)
Haptophyceae						
ANT-Roth-MECl-44	2	Band 13	–	–	*Phaeocystis jahnii* (AF163148)	531/534 (99%)
Cercozoa						
ANT-Roth-MECl-13	1	–	–	–	*Ebria tripartita* (DQ303923)	543/544 (99%)
ANT-Roth-MECl-73	1	–	U.euk. clone DSGM-52 (AB275052)	503/506 (99%)	*Cryothecomonas aestivalis* (AF290539)	482/512 (94%)
ANT-Roth-MECl-31	1	–	U.mar.euk. clone NOR46.14 (DQ314811)	520/540 (95%)	*Cryothecomonas aestivalis* (AF290539)	515/540 (94%)
ANT-Roth-MECl-14	2	Band 4	U.mar.euk. clone NOR46.27 (DQ314814)	537/542 (99%)	*Cryothecomonas longipes* (AF290540)	522/542 (96%)
ANT-Roth-MECl-15	1	Band 4	U.euk. isolate BS_DGGE_Euk-4 (DQ234284)	540/543 (99%)	*Cryothecomonas longipes* (AF290540)	536/543 (99%)
ANT-Roth-MECl-23	6	Band 6	U.mar.euk. clone NOR46.14 (DQ314811)	543/543 (100%)	*Cryothecomonas aestivalis* (AF290539)	538/543 (99%)
Ciliophora						
ANT-Roth-MECl-91	1	–	U.euk. clone SCM16C17 (AY665055)	520/525 (99%)	*Salpingella acuminata* (EU399536)	463/466 (99%)
ANT-Roth-MECl-21	2	Band 5	U.mar.euk. clone SA2_1B7 (EF527117)	393/434 (90%)	*Hartmannula derouxi* (AY378113)	386/430 (89%)
Dinophyceae						
ANT-Roth-MECl-36	3	Band 11	U.mar.euk. clone E4-160 (EU078319)	515/527 (98%)	*Prorocentrum micans* (EF492511)	499/536 (93%)
ANT-Roth-MECl-34	1	–	U.mar.euk. clone SIF_1E11 (EF527103)	523/536 (97%)	*Dinophyceae* sp. RS-24 (AY434686)	509/536 (94%)
ANT-Roth-MECl-50	1	–	–	–	*Gymnodinium catenatum* (DQ779990)	528/536 (98%)

Table 1. Continued.

Group and OTU*	*N*†	DGGE id.‡	Closest BLAST match (accession number)§	Query/similarity¶	Closest cultivated BLAST match (accession no.)‖	Query/similarity¶
ANT-Roth-MECl-96	1	–	U.mar.euk. clone SIF_4E8 (EF527085)	522/536 (97%)	*Pentapharsodinium tyrrhenicum* (AF022201)	518/536 (96%)
ANT-Roth-MECl-101	7	Band 12	U.mar.euk. clone FV_18CilB5 (DQ310298)	521/536 (97%)	*Gyrodinium spirale* (AB120001)	497/511 (97%)
ANT-Roth-MECl-46	8	Band 14	U.mar.euk. clone E3-61 (EU078300)	525/526 (99%)	*Gyrodinium rubrum* (AB120003)	509/510 (99%)
Metazoa						
ANT-Roth-MECl-32	1	Band 9	Undescribed mertensiid sp. 3 (AF293681)	533/537 (99%)	*Mnemiopsis leidyi* (AF293700)	529/537 (98%)
ANT-Roth-MECl-56	3	Band 15	–	–	*Lepidonotus sublevis* (AY894301)	554/556 (99%)
ANT-Roth-MECl-107	1	Band 16	–	–	*Pista cristata* (AY611461)	485/526 (92%)
ANT-Roth-MECl-59	3	–	–	–	*Euphausia superba* (AY672801)	558/558 (100%)
ANT-Roth-MECl-53	1	–	U. mar.euk. clone E1-10 (EU078274)	525/527 (99%)	*Scambicornus* sp. (AY627011)	497/536 (92%)
ANT-Roth-MECl-62	4	Band 17	–	–	*Metridia gerlachei* (AY118076)	516/516 (100%)
ANT-Roth-MECl-63	2	Band 18	–	–	*Calanoides acutus* (AF367712)	531/532 (99%)

*OTU determined as sequences with 97% similarity. Sequences of OTUs in ascending order correspond to NCBI accession numbers FJ985878–FJ985912.
†Number of clones per OTU.
‡Corresponding band in the eukaryote DGGE.
§Closest match from the NCBI database and accession number.
¶Query sequence coverage and percentage similarity.
‖Closest cultivated NCBI match and accession number.

U1406R as a sequencing primer, which yielded partial 16S rRNA gene sequences of approximately 800 bp covering the 16S rRNA gene from approximately 460 to 1270 relative to the nucleotide positions in *E. coli* rRNA gene.

All sequences were checked manually using CHROMAS v.2.3.1. The closest match for each sequence was obtained using NCBI BLAST (http://www.ncbi.nlm.nih.gov/BLAST) and included in the phylogenetic analysis. Sequences that did not yield an unambiguous match in the database were considered as 'suspected chimeric sequences' and were checked online at Ribosomal Database Project II 8.1 CHIMERA CHECK program (http://rdp8.cme.msu.edu/cgis/chimera.cgi?su=SSU) and removed when required. MOLECULAR EVOLUTIONARY GENETICS ANALYSIS (MEGA) version 4.0 (Tamura *et al.*, 2007) and its add-in CLUSTALW were used to align the DNA sequences. After alignment, the sequences were trimmed to remove non-overlapping ends. An unrooted neighbor-joining tree was created based on the maximum composite likelihood algorithm (Hartl *et al.*, 1994; Zhu & Bustamante, 2005). Branch strength was tested with 1000 bootstrap permutations (Felsenstein, 1985). We defined operational taxonomic units (OTUs) as sequences with at least 97% similarity, a cutoff value commonly used in microbial diversity studies. Sequence similarity was determined by pairwise sequence alignment in CLONE MANAGER, version 6 (Scientific & Educational Software). In the phylogenetic tree, OTUs are classified at the taxonomic phylum and class level as deduced from sequences added from the NCBI database. All the sequences presented in this study have been submitted to NCBI database under accession numbers FJ985878–FJ985976.

Results

Environmental variables

The Ryder Bay sea ice data showed the disappearance of sea ice at the end of December. As a result, the study site was ice free throughout our study period (Fig. 1a). CTD data (Fig. 1b) indicated salinity and density stratification of the upper water column throughout January: surface salinity and wind speed measured at our sampling site indicated a first period (*Jd.* 20–32) characterized by relatively low wind speeds [averaging 3.0 m s^{-1}; see fig. 2b in Buma *et al.* (2001)] and

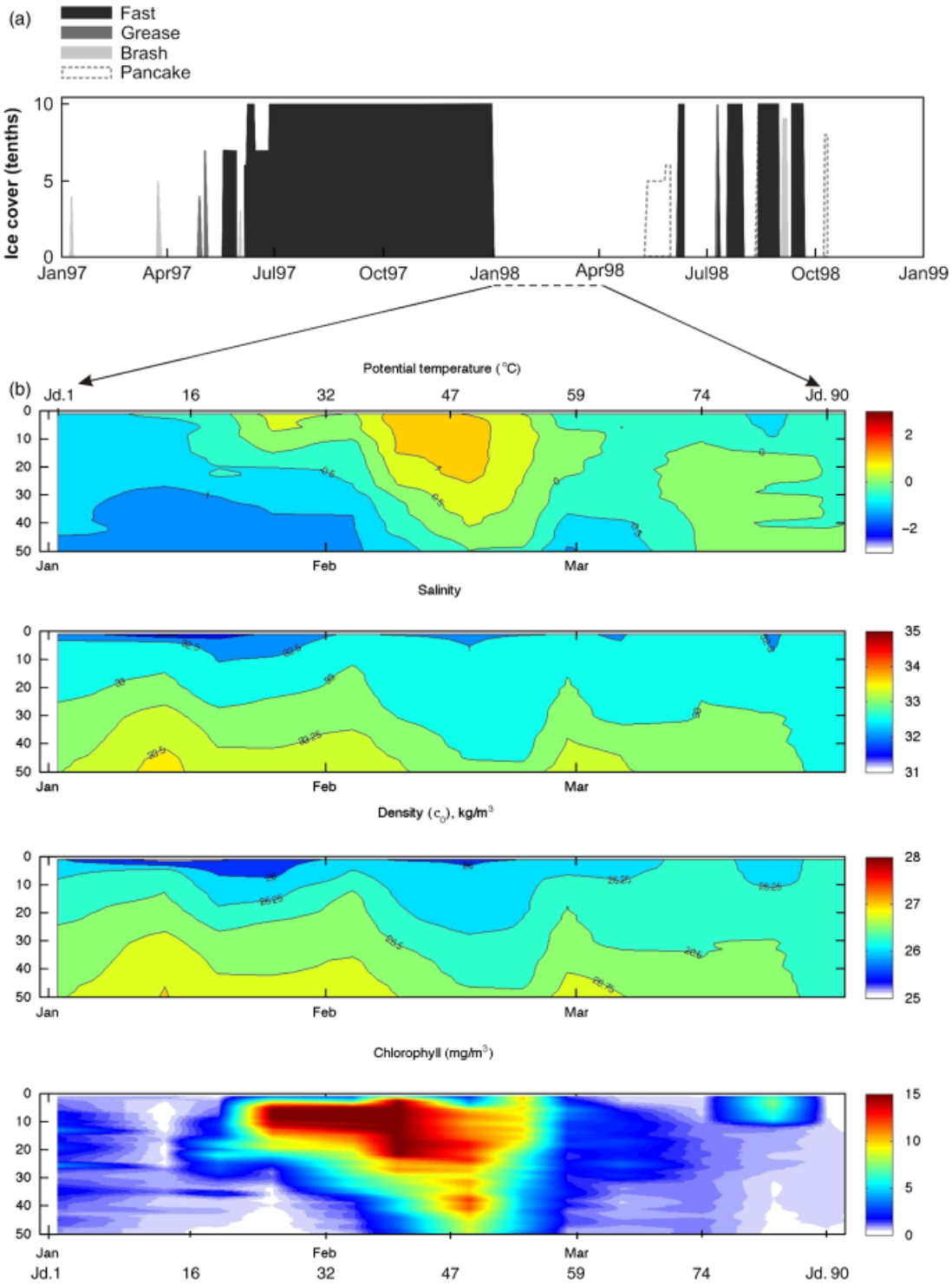

Fig. 1. (a) Ryder Bay sea ice coverage observed from January 1997 to January 1999 by the meteorological station (BAS). (b) CTD profiles from Ryder Bay for water temperature (°C), salinity (‰), density (kg m^{-3}) and chlorophyll (mg m^{-3}) concentrations measured from January 1998 to April 1998. *Jd.*, Julian days are indicated on the upper and under horizontal axes.

low surface salinities (averaging 31.2 psu). This caused salinity stratification of the upper water column (Fig. 1b), with steep salinity and density gradients in the upper 10 m. At the beginning of February, CTD profiles revealed increased surface salinity and density as well as decreased average water temperatures. This second period was

initiated on *Jd*. 33 by the highest wind speed measured during the sampling period (11.7 m s^{-1}), resulting in the breakdown of surface stratification and an immediate increase in surface water salinity from 32.0 psu on *Jd*. 32 to 32.4 psu on *Jd*. 33 (Fig. 1b). Thereafter, the average wind speed was 6.2 m s^{-1} and surface salinity remaining 32.4 psu on average. From mid February onwards, occasional and short periods of weak meltwater stratification occurred. However, several high wind events (> 9 m s^{-1}) observed throughout the second period likely prevented the re-establishment of pronounced surface stratification.

Dynamics of the micro-eukaryotic community

The chlorophyll *a* (chl *a*) data (Fig. 1b) indicated subsurface phytoplankton bloom formation starting the second half of January (Fig. 1b). While initially decreased chl *a* was found in the upper melt water layer, the wind-induced mixing event in the beginning of February (*Jd*. 33 and onwards) caused a more homogenous distribution of the water column. Community shifts and dynamics of the eukaryotes in the 10–200 μm size fraction over time and depth were revealed by DGGE analysis (Fig. 2a). In addition to the $>$ 10-μm samples, four 2–10-μm size-fractionated samples of *Jd*. 20, 31, 41 and 58 were included for comparison. The community fingerprint revealed a temporal variability in band patterns, with a pronounced transition in the micro-eukaryotic community composition occurring between *Jd*. 31 and 37. Here, the disappearance of several bands (e.g. band 3, 5 and 6) and the subsequent appearance of bands 4 and 11 were evident. Up to *Jd*. 33, we also observed a clear stratified micro-eukaryotic community characterized by different DGGE patterns when sampled at different depths. After *Jd*. 33, the band patterns obtained from different depths were more similar as reflected in the dendrogram (Fig. 2b). Samples from days 42 and 52 collected at different depths (0, 5 and 10 m) formed clusters in accordance with the sampling time (42 and 52, Fig. 2b), while samples collected earlier mainly clustered according to depth and secondly according to time (e.g. clusters 31-10-10 and 33-10-10 and clusters 31-0-10, 31-5-10 and 33-0-10). Samples collected before *Jd*. 33 at 10 m depth (D cluster) showed higher similarity to the samples collected later (*Jd*. 37–58, M cluster), rather than to their corresponding surface samples (S cluster, Fig. 2b).

The highest value of the gradient length in an explorative indirect unimodal DCA was < 3, indicating that variability could best be explained by linear ordination (Kent & Coker, 1992). We therefore applied RDA to analyze the variation in our sample set. The ordination analysis was presented as an RDA triplot (Fig. 3), which revealed several clusters that approximated the clusters obtained in the dendrogram (S and M in Fig. 2b.). Two major groups were distinguished: one consisting of samples collected before and one containing samples collected after *Jd*. 33. Furthermore, before *Jd*. 33 samples showed further subgrouping according to collection depth, whereas in the other group further clustering was less evident (Fig. 3). The 2-μm samples were located separately in the upper end of the triplot. The significance of the environmental variables in explaining the observed variation in our data set was tested using Monte Carlo's unrestricted permutation test (1000 permutations). RDA significantly ($P = 0.001$) explained 34% of the variation in our data set. Each variable was tested separately; the environmental variables stratification (water column) and average wind velocity significantly explained most of the variation and appeared to be responsible for the separation between the samples collected before and after *Jd*. 33.

Sequencing of the 18S rRNA gene clone libraries generated from the 10-μm size fractionated samples and from the 2-μm sample 58-0-2 provided information on DGGE band identity. Only bands with at least two clones with similar migration patterns and sequence identities were considered as 'identified' and annotated with a number in the gel. The lower bands (15–18, Table 1) were related to metazoan sequences. Slower migrating bands, confined in the upper part of the gel, were generally diatom-related sequences, while bands from the lower mid part of the gel contained sequences related to dinoflagellates, haptophytes, cercozoans and *Cryothecomonas* sequences. Bands identified as *Gyrodinium rubrum* and *Gyrodinium spirale* were present throughout the survey and at all depths. The composition of the diatom community shifted over time. Initially, *Actinocyclus curvulatus* (band 3) and band *x* (an unidentified *Stramenopile*) dominated the community. These were replaced by *Thalassiosira tumida* (band 8)- and *Eucampia antarctica* (band 1)-related 18S rRNA gene fragments after stratification breakdown ($>$ *Jd* 33). *Cryothecomonas* spp. were identified in bands 4 and 6. On a temporal scale, *Cryothecomonas aestivalis* was present from days 28 to 42 and shortly complemented by *Cryothecomonas longipes* from days 41 to 47.

Eukaryotic species composition

Eukaryotic sequences were divided over six phyla: *Alveolata* (*Dinophyceae* and *Ciliphora*), *Haptophyceae*, *Cercozoa*, Stramenopiles, Metazoa and one cluster related to *Telonema* sp., an unclassified Eukaryota, (Table 1). We identified 35 OTUs; the Stramenopiles were most diverse, with 12 distinct OTUs, which included centric and pennate diatoms. The OTUs related to centric diatoms showed the highest sequence similarities to sequences of *A. curvulatus*, *T. tumida*, *Ditylum brightwellii, Porosira pseudodenticulata*, *Chaetoceros rostratus*, *E. antarctica* and to a lesser extent *Coscinodiscus* sp. GGM-2004. The pennate diatoms were represented by clones related to *Nitzschia longissima*, *Fragilariopsis cylindrus* and *Pseudo-nitzschia pungens*. Alveolates were represented

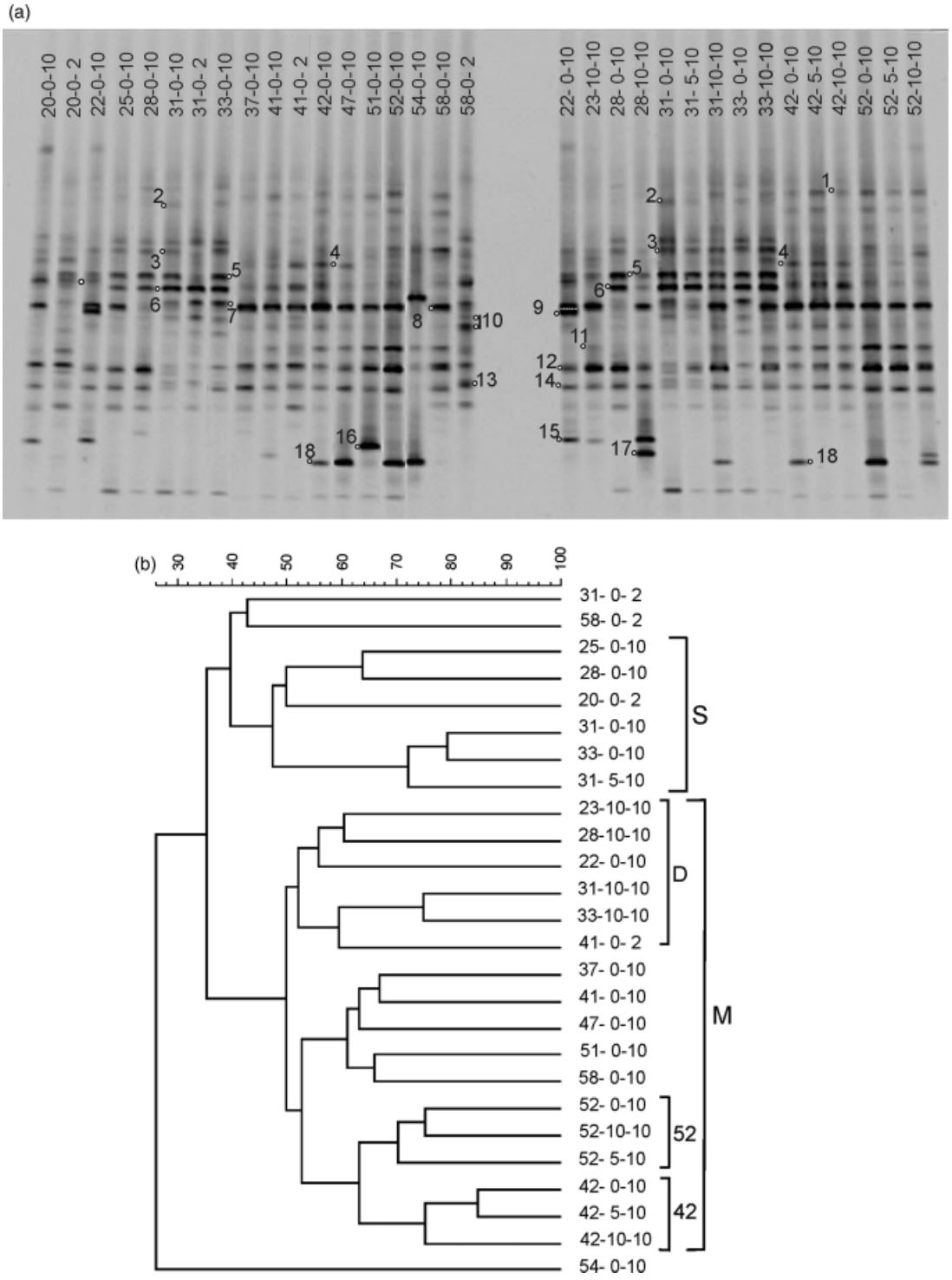

Fig. 2. (a) DGGE image of partial 18S rRNA gene fragments of samples collected over time and at different depths. (b) Dendrogram generated for similarities in band patterns (Dice similarity coefficient). Sample codes: sampling day–sampling depth–size fraction; numbers within the gel refer to bands identified by sequencing efforts (Table 1). Cluster codes areas follows: S, stratified; M, mixed; D, deep.

by six dinoflagellate-related OTUs and two OTUs related to the *Ciliophora*. The dinoflagellate sequences of Ryder Bay showed the highest similarity to sequences of *Prorocentrum micans*, *Dinophyceae* sp. RS-24, *Gymnodinium catenatum*, *Pentapharsodinium tyrrhenicum*, *G. rubrum* and *G. spirale*. The 18S rRNA gene fragments identified as metazoans were

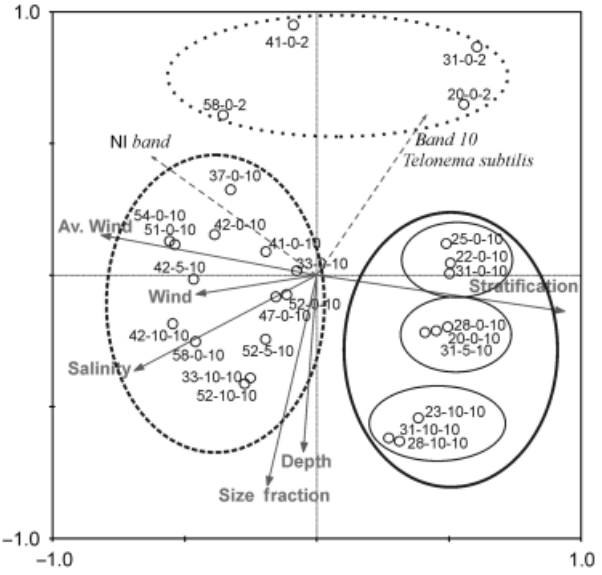

Fig. 3. RDA triplot generated for the 18S rRNA gene community fingerprints. Environmental variables are indicated by gray arrows; species with 50–100% fit by dashed arrows (NI, not identified); samples by rounds (sample codes as in Fig. 2); major clusters are indicated by the ellipses (full, dotted and dashed lines).

affiliated to four typical Antarctic crustaceans (*Euphausia superba*, *Scambicornus* sp., *Calanoides acutus* and *Metridia gerlachei*), two polychaetes (*Pista cristata*, *Lepidonotus sublevis*) and a cnidarian (*Mnemiopsis leidyi*). Several cloned fragments proved to share most identity with cercozoan sequences, which included *C. longipes*, *C. aestivalis* and *Ebria tripartita*. One OTU was identified as a haptophycean, most similar to *Phaeocystis jahnii*.

Dynamics of the bacterial community

The bacterial community was subjected to DGGE analysis by amplifying a ~450-bp fragment of the 16 rRNA gene from the smallest size fraction (0.2–2 μm) of the samples collected in Ryder Bay. However, due to a lack of sufficient quantities of DNA in this size fraction, we could only analyze a reduced (eight out of 15) sample set. DGGE analysis revealed the temporal variation in the bacterial community and differences in band patterns from samples collected at different depths (Fig. 4). A shift in the band pattern appeared after *Jd*. 37, notably in the upper part of the gel (+ and *, Fig. 4). The upper band (+) was only apparent in samples collected after *Jd*. 37, while the lower band (*), which was present in the surface layer after *Jd*. 37, was only present before that date in the deeper samples collected at 5 or 10 m depth. In samples 41-0, 54-0, 31-5 and 43-5, the quadruplet set of bands (#) in the upper end of the gel disappeared temporarily. Given the limited number of subsurface samples available (5, 10 m), similarity analysis was only performed on surface samples (Fig. 4b). This analysis revealed higher similarity for the bacterial band patterns as compared with the eukaryotic samples. All band profiles shared at least 60% similarity, except for the divergent band pattern of sample 47-0. Two main clusters emerged in accordance with the sampling time: samples collected from *Jd*. 20 to 37 (cluster S) and samples collected from *Jd*. 41 to 58 (cluster M). Samples within these clusters showed high similarity to each other. All except one sample (33-0-2) had > 80% similarity in the first cluster and > 70% similarity in the second cluster.

RDA of species variation (bands) and environmental variable significantly explained 36.1% of the variation in our data set (Monte Carlo's permutation test, $P = 0.001$). The variation along the first axis, which explained 19.9% variation ($P = 0.001$), mostly correlated with the environmental variable *stratification*. Separate RDA analysis performed for each variable revealed that the variables *stratification* and *average wind* significantly explained 18.2% and 15.4% of the variation ($P = 0.001$). Three main clusters emerged in the RDA triplot (Fig. 5) that separated according to time, as in the dendrogram, and secondly according to depth. The environmental variable *stratification* explained the largest part of the variation in the data set, roughly separating samples collected before and after *Jd*. 37.

Bacterial species composition

A total of 375 partial 16S rRNA gene sequences were analyzed, revealing the presence of members belonging to the *Gammaproteobacteria*, *Betaproteobacteria*, *Alphaproteobacteria*, *Actinobacteria* and to the *Cytophaga–Flavobacterium–Bacteroides* (CFB) group; 24 sequences were closely related to 16S-like chloroplasts/plastids of eukaryote origin (Fig. 6). We identified a total of 64 OTUs (FJ985913–FJ985976). The CFB phylum appeared to be the most diverse, with 22 OTUs, and included sequences related to *Polaribacter* sp., *Flavobacterium* sp., *Bacteroidetes* sp. and *Cytophagales* sp. Sequences related to the *Gammaproteobacteria* consisted of 21 OTUs with members of the SAR 86 cluster, *Psychromonas* sp., *Pseudoalteromonas* sp., *Pseudomonas* sp., *Glaceicola* sp. and *Psychrobacter* sp. In the phylogenetic tree, one *Gammaproteobacteria*-related OTU (Cl 5-37, *Psychrobacter* sp.) was positioned separately from the main cluster, between the CFB and the chloroplast/plastid phyla. Sequences from this cluster were not chimeras and did not reveal any inconsistencies. The *Alphaproteobacteria* included sequences related to the *Pelagibacter ubique* member of the SAR 11 cluster and *Roseobacter* sp. The clone library revealed a few sequences related to the *Actinobacteria* and *Betaproteobacteria*. The relative distribution of bacterial sequences (excluding sequences of chloroplast or plastid origin) was

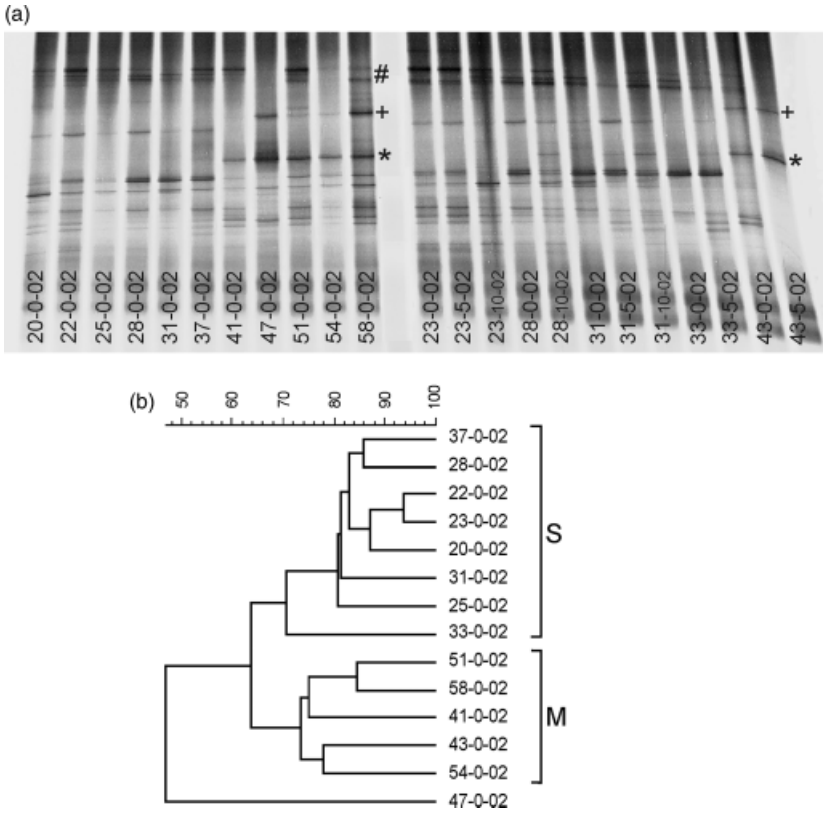

Fig. 4. (a) DGGE image of partial 16S rRNA gene fragments from environmental samples collected over time. (b) Dendrogram generated for similarities in the DGGE band patterns. Codes as in Fig. 2; the bands mentioned in text are indicated by symbols.

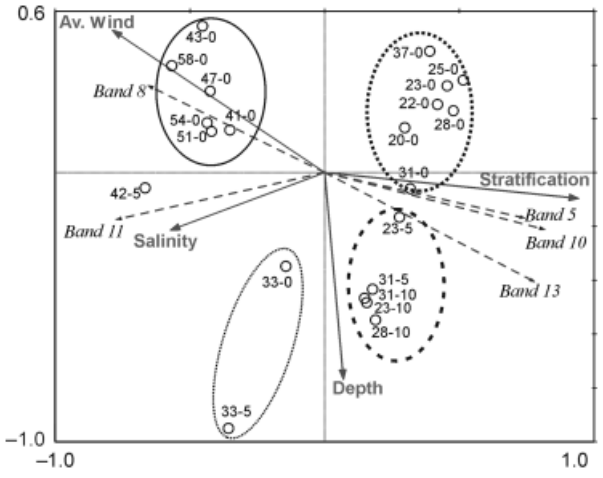

Fig. 5. RDA triplot generated for 16S rRNA gene DGGE band patterns. Species are unidentified and therefore numbered according to DGGE band position. Codes used are as in Fig. 2.

calculated for the entire clone library (343 clones, *total*) and for each sample used to generate clone libraries (Fig. 7). OTUs were pooled into subclusters according to the main branches found in the phylogenetic tree. For example, the OTUs 6-22, 1-60 and 5-38 formed a cluster related to *Psychromonas* sp., yielding 22 clusters. The pie chart representing the entire clone library resolved at the phylum level (outer ring of *Total* in Fig. 7) revealed that the CFB (green and gray gradients) covered 41.7% of the sequences, while the second most dominant phylum belonged to the *Gammaproteobacteria* (35.7%) and the third to the *Alphaproteobacteria* (19.2%). At the cluster level, gamma-1 (16.9%), *Polaribacter irgensii* (16.6%), *Flavobacter*-3 (13.1%) and SAR 11 (10.1%) sequences dominated the clone library. Clone libraries of samples collected from *Jd*. 22 to 28 revealed that *Gamma-* and *Alphaproteobacteria*-related clones dominated initially, with members of the SAR11 and gamma-1 clusters forming the largest part of each of these phyla. The sample collected on *Jd*. 23 from 10-m depth showed strong differences with the surface samples. At 10-m depth, clones related to the CFB phylum dominated the clone library with the *P. irgensii* and *Flavobacter*-2 clusters. The diversity of the *Gammaproteobacteria* was reduced to two clusters, while all other samples harbored sequences from at least four *Gammaproteobacteria* clusters. The *Alphaproteobacteria* clones remained abundant at 10 m depth, but sequences belonging to the *Roseobacter*1 cluster dominated. Clone libraries of samples collected after *Jd*. 28 revealed a strong decrease in *Alphaproteobacteria*, while CFB-related

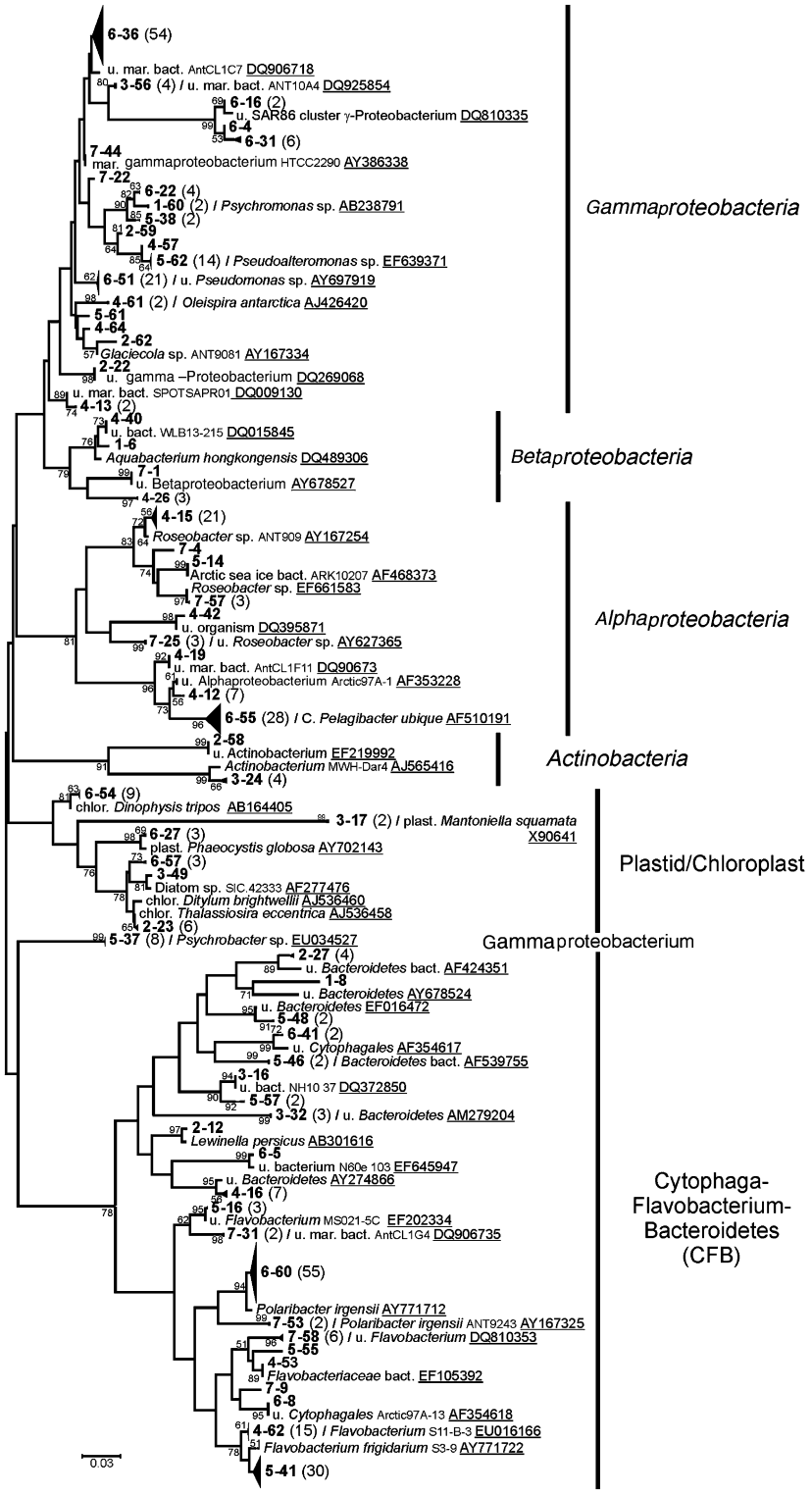

Fig. 6. Neighbor-joining phylogenetic tree showing the position of partial 16S rRNA gene sequences obtained from the generated clone libraries. The clone codes are shown in bold; the number of clones per OTU is indicated in parentheses; sequences were provided as 'ANT-Roth-umbCl-***clone code***' to the NCBI database in ascending order: [1–6 to 7–58] correspond to [FJ985913–FJ985976].

sequences strongly increased, forming 40–65% of the clones. In these samples, the *Gammaproteobacteria* clones formed the other large portion of the clone library, except in samples 51-0, where members of the *Flavobacterium3* cluster constituted 65% of the library. Overall, the clone distribution indicated that *Gamma-* and *Alphaproteobacteria* dominated the surface water samples under stratified conditions (before *Jd*. 33) and differences could be detected between samples

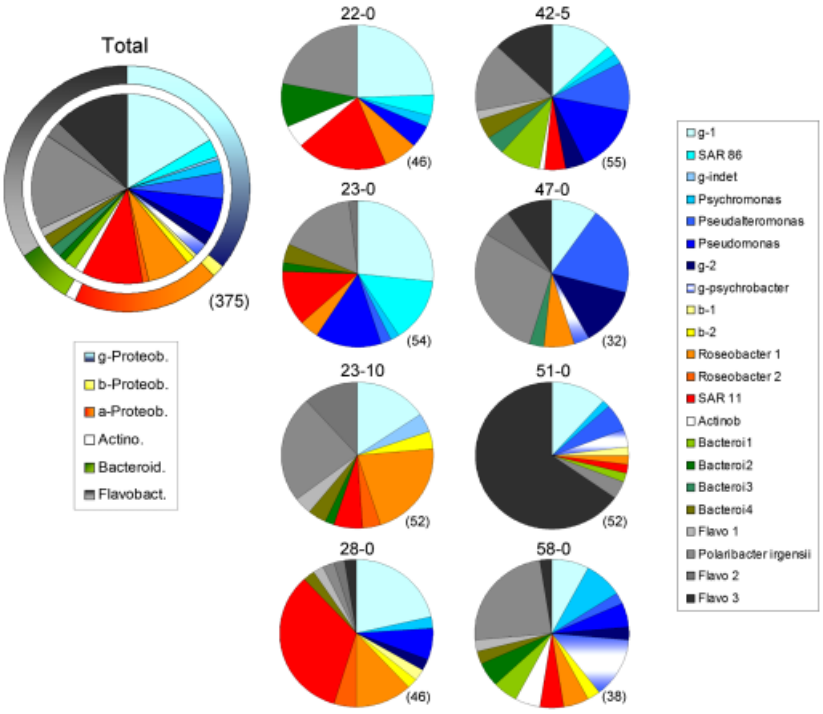

Fig. 7. Relative distribution of bacterial clones recovered for all sequences (total) and per cloned sample. The distribution of clones is represented per OTU cluster (pie chart) per bacterial phylum (outer ring). The total clones sequenced are indicated in parentheses next to the pie chart. Color codes used: shades of blue, *Gammaproteobacteria* (g); yellow, *Betaproteobacteria* (b); orange to red, *Alphaproteobacteria*; white, *Actinobacteria*; green and gray, CFB. g, *Gammaproteobacteria*; undet., undetermined; b, *Betaproteobacteria*; Actino., *Actinobacteria*; Bacteroi., *Bacteroidetes*; Flavo., *Flavobacteria*.

collected at different depths in this period, with a strong influx of CFB clones at 10 m depth. This was found to be consistent with an increased dominance of CFB clones in surface samples after stratification breakdown.

Discussion

The identification of 18S rRNA gene fragments (DGGE bands) provided an insight into the species dynamics of the Ryder Bay community from January to February 1998. Sequencing of the amplified 18S rRNA gene fragments revealed that most clones were related to Stramenopiles and included species that were also observed by microscopy analysis (Buma *et al.*, 2001). Moreover, in Buma *et al.* (2001), analysis of several taxon-specific markers showed that the diatom-specific pigment fucoxanthin had the highest concentration (apart from chlorophyll *a*) throughout the sampling period. Microscopic analysis confirmed the dominance of diatoms, especially of *Thalassiosira* sp., *Pseudonitzschia* sp. and *Eucampia* sp. species. *Nitzschia* sp. and *Chaetoceros* sp. were also detected by 18S rRNA gene sequencing, while the diatoms *Rhizosolenia* sp. and *Odontella* sp. were only detected by microscopy (Buma *et al.*, 2001). Species related to *Actinocyclus* sp., *Coscinodiscus* sp., *Porosira* sp. and *Ditylum* sp. were only detected by molecular analysis. Flagellates identified by microscopy consisted partly of prasinophytes, judging from the presence of chlorophyll *b* and prasinoxanthin, as measured by HPLC (Buma *et al.*, 2001). Sequence and DGGE analysis revealed a group of flagellate species related to *Cryothecomonas* sp. that was represented by six OTUs. It has to be emphasized that more flagellate sequences might have been present in the 2–10-μm size fraction, but unfortunately, the DNA yield in this size fraction was often too low for further processing. In our study, DGGE analysis revealed a shift in eukaryotic band patterns after wind-induced vertical mixing. However, this shift was overlooked by the pigment data (in Buma *et al.*, 2001) as the shifts mainly occurred at the species level, with diatom species dominating throughout the survey period. Because each of the techniques has its own benefits and drawbacks, none of which captures the full diversity, a combination of these techniques still appears to be the best way to describe microbial community dynamics. The 18S rRNA gene analysis may reveal species that are missed by microscopy and pigment analysis, but is hampered by a relatively low number of sequences per sample. Possibly, the use of next-generation high-throughput sequencing techniques such as 454 life sequencing (Sogin *et al.*, 2006) will provide the numbers of sequences required to study the full microbial diversity.

Upper water column stabilization by melt water input appeared to be responsible for shaping the surface eukaryotic community during our survey in Ryder Bay, which is in agreement with other studies performed in the Antarctic (Kang *et al.*, 2001; Dierssen *et al.*, 2002) and recent data by Annett *et al.* (2010) that used classical microscopy and pigment analysis to study phytoplankton dynamics in Ryder Bay. The eukaryotic community analysis by DGGE revealed

significant differences in band patterns from the surface to 10 m depth in the stratified water column. Secondly, our data showed that stratification breakdown during summer caused rapid shifts in both eukaryote and bacterial communities. The first high wind event (*Jd*. 33) induced destruction of the stabilized surface water layer and a rapid shift in the eukaryotic community, as revealed by the appearance of novel bands in the surface samples. Some of these bands (e.g. 1, *E. antarctica*; 4, *C. longipes*; 8, *T. tumida*) were present in the 10-m depth samples collected during the stratified period. Wind-induced vertical mixing caused an increase in surface salinity and a redistribution of eukaryotic species over the upper water column that remained stable thereafter. Microscopy cell counts performed on the surface samples indicated a fourfold increase in the average diatom numbers during the mixing period ($15.2–68.0 \times 10^4$ cells L^{-1} (Buma *et al*., 2001), which agrees with the observed chlorophyll increase in this period (Fig. 1b). In our study, diatoms were dominating, irrespective of the occurrence of stratification or deep mixing. Thus, our data do not support earlier studies where phytoflagellate increase was associated with low surface salinity (Moline & Prézelin, 1996) or deep vertical mixing (Arrigo *et al*., 1999). Moreover, the increase in chl *a* observed during mixing must have been mainly due to an increase in diatoms, judging from elevated fucoxanthin levels using HPLC pigment fingerprinting (Buma *et al*., 2001). As calculated in Buma *et al*. (2001), prasinophytes (the major nondiatom group) constituted no more that 3% of the total chl *a* pool, while hexanoyloxyfucoxanthin (indicative of prymnesiophytes) and alloxanthin (indicative of cryptophytes) were not detected. This contrasts with the study of Annett *et al*. (2010), who demonstrated high prymnesiophyte (*Phaeocystis antarctica*) abundance during the summer months, between 2004 and 2007. In other words, phytoflagellate groups were highly under-represented during our survey, compared with other years. As a result, phytoflagellates may not have been able to surpass diatom growth, even when conditions would favor their dominance.

The effect of stratification vs. mixing was less apparent for the bacterial community, although two clusters emerged from the DGGE data and subsequent analyses. The shift in the bacterial community composition did not occur simultaneously with the mixing event and the shift in the microeukaryotic community at *Jd*. 33. A shift was only apparent in the next sample (*Jd*. 37), 4 days after the mixing event, suggesting that the bacterial response occurred somewhere between *Jd*. 34 and 37. Bacteria generally respond to changes in phytoplankton growth and species composition with a lag phase. Billen & Becquevort (1991) reported a 1-month delay in the response of Antarctic bacterial production to the phytoplankton spring bloom. This delay was attributed to the size and composition of the available DOM pool. More recently, delays in bacterial diversity responses to increased primary production proved to vary according to the bacterial species present. Bacteria belonging to the CFB revealed a rapid response to increased primary productivity with increasing species richness, while members of the *Alphaproteobacteria* showed a U-shaped species richness response to increased primary productivity (Horner-Devine *et al*., 2003).

Sequencing of the 16S rRNA gene revealed that the smallest bacterioplankton size fraction was dominated by CFB- and *Gammaproteobacteria*-related sequences. This is in agreement with previous findings of other Antarctic marine studies using molecular approaches (Glöckner *et al*., 1999; Simon *et al*., 1999; Abell & Bowman, 2005b; Gentile *et al*., 2006). CFB members have been reported to react rapidly to increases in primary production (Horner-Devine *et al*., 2003; Abell & Bowman, 2005b). This fits the observation of increased CFB clone numbers in surface samples collected during the mixing period, which coincides with the redistribution of the phytoplankton bloom over the upper 25 m of the water column (Fig. 1b), causing an increase in diatom abundance. In contrast, *Alphaproteobacteria*, which were found in all our samples, and known to be ubiquitous in the marine environment and well represented in the Southern Ocean and Antarctic coastal sites (Simon *et al*., 1999), did not form a dominant fraction in our samples. Previous studies indicate that *Alphaproteobacteria* react with a lag phase to increased primary productivity (Horner-Devine *et al*., 2003). In the West Antarctic Peninsula, *Roseobacter* spp., representatives of the *Alphaproteobacteria*, proved to increase throughout the austral summer from December to March (Ducklow *et al*., 2007). Possibly, the *Alphaproteobacteria* are outcompeted by CFBs at the onset of the spring bloom, but increase later in population size when the phytoplankton bloom is decaying. In support of this, Abell & Bowman (2005a) conducted mesocosm experiments to study the colonization of phytoplankton detritus by bacteria and observed an initial colonization by members of the CFB, followed by *Alpha-* and *Gammaproteobacteria*. The relative distribution of sequences in our survey revealed elevated numbers of *Alphaproteobacteria* sequences during the stratified period. The *Alphaproteobacteria* may have benefited from decaying ice algae released from melting sea ice and transformed DOM in the upper layer.

In conclusion, our study revealed that the application of molecular tools provided a relatively efficient method to detect shifts in the community composition in relation to the physical state of Antarctic surface waters. Shifts in the eukaryotic community were rapidly followed by a shift in the bacterial community during wind-induced breakdown of melt water-related surface stratification in Ryder Bay, validating our hypothesis that alterations in Antarctic

surface water properties shape marine microbial communities. As climate is changing rapidly in polar regions, including the Antarctic Peninsula region (Ducklow *et al.*, 2007; Shepherd & Wingham, 2007), the resultant alterations in salinity and temperature stratification as well as the average wind speeds will not only affect eukaryotic but also prokaryotic marine coastal communities.

Acknowledgements

We would like to thank Karin de Boer for the sample collection and Jolanda Brons for technical assistance. Moreover, we are very grateful to BAS for accommodating our field campaign. This field campaign was financed by the Dutch Committee for Antarctic Research (Dutch Science Foundation, Project no. 751-499-02).

References

Abell GCJ & Bowman JP (2005a) Colonization and community dynamics of class *Flavobacteria* on diatom detritus in experimental mesocosm based on Southern Ocean seawater. *FEMS Microbiol Ecol* **53**: 379–391.

Abell GCJ & Bowman JP (2005b) Ecological and biogeographic relationships of class *Flavobacteria* in the Southern Ocean. *FEMS Microbiol Ecol* **51**: 265–277.

Annett AL, Carson DS, Crosta X, Clarke A & Ganeshram RS (2010) Seasonal progression of diatom assemblages in surface waters of Ryder Bay, Antarctica. *Polar Biol* **33**: 13–29.

Arrigo KR, Robinson DH, Worthern DL, Dunbar RB, DiTullio GR, VanWoert M & Lizotte MP (1999) Phytoplankton community structure and the drawdown of Nutrients and CO_2 in the Southern Ocean. *Science* **283**: 365–367.

Beszteri B, Ács É & Medlin LK (2005) Ribosomal DNA sequence variation among sympatric strains of the cyclotella meneghiniana complex (Bacillariophyceae) reveals cryptic diversity. *Protist* **156**: 317–333.

Billen G & Becquevort S (1991) Phytoplankton-bacteria relationship in the Antarctic marine ecosystem. *Polar Res* **10**: 245–253.

Buma AGJ, de Boer MK & Boelen P (2001) Depth distribution of DNA damage in Antarctic marine phyto- and bacterioplankton exposed to summertime UV radiation. *J Phycol* **37**: 200–208.

Casamayor EO, Massana R, Benlloch S, Øvreås L, Díez B, Goddard VJ, Gasol JM, Joint I, Rodríguez-Valera F & Pedrós-Alió C (2002) Changes in archaeal, bacterial and eukaryal assemblages along a salinity gradient by comparison of genetic fingerprinting methods in a multipond solar saltern. *Environ Microbiol* **4**: 338–348.

Clarke A, Meredith MP, Wallace MI, Brandon MA & Thomas DN (2008) Seasonal and interannual variability in temperature, chlorophyll and macronutrients in northern Marguerite Bay, Antarctica. *Deep Sea Res Pt II* **55**: 1988–2006.

Dierssen HM, Smith RC & Vernet M (2002) Glacial meltwater dynamics in coastal waters west of the Antarctic peninsula. *P Natl Acad Sci USA* **99**: 1790–1795.

Díez B, Pedrós-Alió C, Marsh TL & Massana R (2001) Application of denaturing gradient gel electrophoresis (DGGE) to study the diversity of marine picoeukaryotic assemblages and comparison of DGGE with other molecular techniques. *Appl Environ Microb* **67**: 2942–2951.

Doyle JJ & Doyle JL (1987) A rapid DNA isolation procedure for small quantities of fresh leaf tissue. *Phytochem Bull* **19**: 11–15.

Ducklow HW, Baker K, Martinson DG, Quetin LB, Ross RM, Smith RC, Stammerjohn SE, Vernet M & Fraser W (2007) Marine pelagic ecosystems: the West Antarctic Peninsula. *Philos T Roy Soc B* **362**: 67–94.

Felsenstein J (1985) Confidence limits on phylogenies: an approach using the bootstrap. *Evolution* **39**: 783–791.

Ferrari VC & Hollibaugh JT (1999) Distribution of microbial assemblages in the central Arctic Ocean Basin studies by PCR/DGGE: analysis of a large data set. *Hydrobiologia* **401**: 55–68.

Frey JC, Angert ER & Pell AN (2006) Assemsment of biases associated with profiling simple, model communities using t-RFLP-based analysis. *J Microbiol Meth* **67**: 9–19.

Gast RJ, Dennett MR & Caron DA (2004) Characterization of protistan assemblages in the Ross Sea, Antarctica, by denaturing gradient gel electrophoresis. *Appl Environ Microb* **70**: 2028–2037.

Gentile G, Giuliano L, D'Aurelia G, Smedile F, Azzaro M, Domenico MD & Yakimov MM (2006) Study of bacterial communities in Antarctic coastal waters by a combination of 16S rRNA and 16S rDNA sequencing. *Environ Microbiol* **8**: 2150–2161.

Glöckner FO, Fuchs BM & Amann RI (1999) Bacterioplankton composition of lakes and oceans: a first comparison based on fluorescence *in situ* hybridization. *Appl Environ Microb* **65**: 3721–3726.

Guillou L, Eikrem W, Chrétiennot-Dinet M-J, Le Gall F, Massana R, Pedrós-Alió C & Vaulot D (2005) Diversity of picoplankton Prasinophytes assessed by direct nuclear SSU rDNA sequencing of environmental samples and novel isolates retrieved from oceanic and coastal ecosystems. *Protists* **155**: 193–214.

Hartl DL, Moriyama EN & Sawyer SA (1994) Selection intensity for Codon bias. *Genetics* **138**: 227–234.

Horner-Devine M, Leibold MA, Smith VH & Bohannan BJM (2003) Bacterial diversity patterns along a gradient of primary productivity. *Ecol Lett* **6**: 613–622.

Janse I, Bok J & Zwart G (2004) A simple remedy against artificial double bands in DGGE. *J Microbiol Meth* **57**: 279–281.

Kang S-H, Kang J-S, Lee S, Chung KH, Kim D & Park MG (2001) Antarctic phytoplankton assemblages in the marginal ice zone of the northwestern Weddell Sea. *J Plankton Res* **23**: 333–352.

Kent M & Coker P (1992) *Vegetation Description and Analysis: A Practical Approach*. Belhaven Press, London, UK.

López-García P, Rodríguez-Valera F, Pedrós-Alió C & Moreira D (2001) Unexpected diversity of small eukaryotes in deep sea Antarctic plankton. *Nature* **409**: 603–607.

Massana R, Pedrós-Alió C, Casamayor EO & Gasol JP (2001) Changes in marine bacterioplankton phylogenetic composition during incubations designed to measure biogeochemically significant parameters. *Limnol Oceanogr* **46**: 1181–1188.

Massana R, Castresana J, Balagué V, Guillou L, Romari K, Groisiller A, Valentin K & Pedrós-Alió C (2004) Phylogenetic and ecological analysis of novel marine Stramenopiles. *Appl Environ Microb* **70**: 3528–3534.

Moline MA & Prézelin BB (1996) Long-term monitoring and analyses of physical factors regulating variability in coastal antarctic phytoplankton biomass, *in situ* productivity and taxonomic composition over subseasonal and interannual time scales. *Mar Ecol Prog Ser* **145**: 143–160.

Moon-van der Staay SY, Wachter De R & Vaulot D (2003) Oceanic 18S rDNA sequences from picoplankton reveal unsuspected eukaryotic diversity. *Nature* **409**: 607–610.

Moreira D & López-García P (2002) The molecular ecology of microbial eukaryotes unveils a hidden world. *Trends Microbiol* **10**: 31–38.

Mura MP, Satt MP & Agustí S (1995) Water-mass influence on summer Antarctic phytoplankton biomass and community structure. *Polar Biol* **15**: 15–20.

Nübel U, Engelen B, Felske A, Snaidr J, Wieshuber A, Amann RI, Ludwig W & Backhaus H (1996) Sequence heterogeneities of genes encoding 16S rRNA in *Paenibacillus polymyca* detected by TGGE. *J Bacteriol* **178**: 5636–5643.

Piquet AM-T, Bolhuis H, Davidson AT, Thomson PG & Buma AGJ (2008) Diversity and dynamics of Antarctic marine microbial eukaryotes under manipulated environmental UV radiation. *FEMS Microbiol Ecol* **66**: 352–366.

Piquet AM-T, Scheepens JF, Bolhuis H, Wiencke C & Buma AGJ (2010) Variability of protistan and bacterial communities in two Arctic fjords (Spitsbergen). *Polar Biol* 1–16. DOI: 10.1007/s00300-010-0841-9.

Richards TA & Bass D (2005) Molecular screening of free-living microbial eukaryotes: diversity and distribution using a meta-analysis. *Curr Opin Microbiol* **8**: 240–252.

Riemann L, Leitet C, Pommier T, Simu K, Holmquist L, Larsson U & Hagström Å (2008) The native bacterioplankton community in the Central Baltic sea is influenced by freshwater bacterial species. *Appl Environ Microb* **74**: 503–515.

Schäfer H, Bernard L, Courties C, Lebaron P, Servais P, Pukall R, Vives-Rego J & Muyzer G (2001) Microbial community dynamics in Mediterranean nutrient-enriched seawater mesocosms: changes in genetic diversity of bacterial populations. *FEMS Microbiol Ecol* **34**: 243–253.

Shepherd A & Wingham D (2007) Recent sea-level contributions of the Antarctic and Greenland ice sheet. *Science* **315**: 1529–1532.

Simon M, Glöckner FO & Amann R (1999) Different community structure and temperature optima of heterotrophic picoplankton in various regions of the Southern Ocean. *Aquat Microb Ecol* **18**: 275–284.

Sogin ML, Morrison HG, Huber JA, Welch DM, Huse SM, Arrieta JM & Herndl GJ (2006) Microbial diversity in the deep sea and the under-explored 'rare biosphere'. *P Natl Acad Sci USA* **103**: 12115–12120.

Speksneijder AGCL, Kowalchuk GA, de Jong S, Kline E, Stephen JR & Laanbroek HJ (2001) Microvariation artifacts introduced by PCR and cloning of closely related 16S rRNA gene sequences. *Appl Environ Microb* **67**: 469–472.

Suzuki MT & Giovannoni SJ (1996) Bias caused by template annealing in the amplification of mixtures of 16S rDNA genes by PCR. *Appl Environ Microb* **62**: 625–630.

Tamura K, Dudley J, Nei M & Kumar S (2007) MEGA4: Molecular Evolutionary Genetics Analysis (MEGA) software version 4.0. *Mol Biol Evol* **24**: 1596–1599.

Ter Braak CJF & Šmilauer P (1998) *CANOCO Reference Manual and User's Guide to Canoco for Windows: Software for Canonical Community Ordination (Version 4.5.2)*. Ithaka, New York.

Van den Wollenberg AL (2007) Redundancy analysis. An alternative for canonical correlation analysis. *Psychometrika* **42**: 207–219.

Zhu L & Bustamante CD (2005) A composite-likelihood method for detecting directional selection from DNA sequence data. *Genetics* **170**: 1411–1421.